


Article

Miscanthus to Biocarbon for Canadian Iron and Steel Industries: An Innovative Approach

Trishan Deb Abhi, Omid Norouzi, Kevin Macdermid-Watts, Mohammad Heidari, Syeda Tasnim and Animesh Dutta * 

School of Engineering, University of Guelph, Guelph, ON N1G 2W1, Canada; tabhi@uoguelph.ca (T.D.A.); Norouzio@uoguelph.ca (O.N.); kmacderm@uoguelph.ca (K.M.-W.); mheidari@uoguelph.ca (M.H.); stasnim@uoguelph.ca (S.T.)

* Correspondence: adutta@uoguelph.ca

Abstract: Iron-based industries are one of the main contributors to greenhouse gas (GHG) emissions. Partial substitution of fossil carbon with renewable biocarbon (biomass) into the blast furnace (BF) process can be a sustainable approach to mitigating GHG emissions from the ironmaking process. However, the main barriers of using biomass for this purpose are the inherent high alkaline and phosphorous contents in ash, resulting in fouling, slagging, and scaling on the BF surface. Furthermore, the carbon content of the biomass is considerably lower than coal. To address these barriers, this research proposed an innovative approach of combining two thermochemical conversion methods, namely hydrothermal carbonization (HTC) and slow pyrolysis, for converting biomass into suitable biocarbon for the ironmaking process. Miscanthus, which is one of the most abundant herbaceous biomass sources, was first treated by HTC to obtain the lowest possible ash content mainly due to reduction in alkali matter and phosphorous contents, and then subjected to slow pyrolysis to increase the carbon content. Design expert 11 was used to plan the number of the required experiments and to find the optimal condition for HTC and pyrolysis steps. It was found that the biocarbon obtained from HTC at 199 °C for 28 min and consecutively pyrolyzed at 400 °C for 30 min showed similar properties to pulverized coal injection (PCI) which is currently used in BFs due to its low ash content (0.19%) and high carbon content (79.67%).

Keywords: biocarbon; hydrothermal carbonization (HTC); slow pyrolysis; pulverized coal injection (PCI); blast furnace (BF); CO₂ emission mitigation; miscanthus



Citation: Deb Abhi, T.; Norouzi, O.; Macdermid-Watts, K.; Heidari, M.; Tasnim, S.; Dutta, A. Miscanthus to Biocarbon for Canadian Iron and Steel Industries: An Innovative Approach. *Energies* **2021**, *14*, 4493. <https://doi.org/10.3390/en14154493>

Academic Editor: Prasad Kaparaju

Received: 15 June 2021

Accepted: 23 July 2021

Published: 25 July 2021

Publisher's Note: MDPI stays neutral with regard to jurisdictional claims in published maps and institutional affiliations.



Copyright: © 2021 by the authors. Licensee MDPI, Basel, Switzerland. This article is an open access article distributed under the terms and conditions of the Creative Commons Attribution (CC BY) license (<https://creativecommons.org/licenses/by/4.0/>).

1. Introduction

Among all steel production routes, the blast furnace (BF) ironmaking process is considered the most popular technology to meet the increasing metal demand worldwide [1,2]. In Canada, about 5.8 Mt of metal is produced by BF ironmaking processes per year, which is approximately 80% of the total Canadian metal production [1].

In this process, carbon in the form of coke (produced by heating coal in the absence of air) ignites and burns in the presence of sub-stoichiometric amount of air to produce carbon monoxide. This carbon monoxide is then used to reduce the metal oxide to metal and make carbon dioxide [3]. Hence, coal is used as the heat source as well as a reduction agent. However, the reliance of the process on coal contributes to catastrophic greenhouse gas (GHG) emissions. BFs consume 12.31 GJ of energy and release 1.8 ton CO₂ for the production of one ton of metal [4,5].

Biomass can be considered a promising renewable alternative for coal. The combustion of biomass does not increase the net atmospheric CO₂ concentration, as it is balanced by the amount of CO₂ the plant absorbs during its lifespan [6]. The use of woody biomass in the ironmaking process has been reported in literature. However, for biomass to be used in BFs, raw materials costs, low O/C ratios, low ash content, and operational challenges all need to be considered and evaluated before implementation [7]. Wing Ng et al. [8] reported

a significant reduction in GHG emission (from 1.55 CO_{2eq}/ton to 0.26 CO_{2eq}/ton) by substituting coal with wood pellets in the ironmaking process. Another research group [9] claimed that direct solid biocarbon injection, produced from hardwood in the furnace, can mitigate more than 20% of GHG emissions. Nidheesh and Kumar [10] provided a review on the environmental impacts of steel production, as well as discussing pathways for increased sustainability, and the potential biomass has for this transition.

Perhaps the main concern with respect to introducing the biomass-derived biochar into the BF is its relatively high ash content. Lead (Pb), zinc (Zn), sodium (Na), potassium (K), sulfur (S), and phosphorous (P) are the main building block elements of ash [11]. The presence of those chemical components significantly affects the BF ironmaking process due to the fouling, slagging, and scaling effects on the boiler surface [12]. This is likely why biocarbon production from high-ash-content agricultural biomass (such as miscanthus, wheat straw, and corn stover) has not been studied as deeply as biomass with low ash content (such as pine saw dust, loblolly pine, and willow) [13]. In addition to high ash content, another obstacle to the use of agricultural waste in the boilers is their low heating value in comparison to coal [14]. As agricultural waste is a considerable resource due to massive production of food in the farms, as well as the ability for crops like miscanthus to be grown perennially on marginal land with low inputs and high sustainability [15], more research is required to overcome the barriers of using them in energy intensive sectors like ironmaking process.

Thermochemical processing of biomass such as hydrothermal carbonization (HTC) and pyrolysis can change the properties such as ash content and heating value of the agricultural biomass to the desired condition. However, it has been shown in a comprehensive review [16] on advances of torrefaction technologies and conventional slow pyrolysis suggest that a degree of uncertainty exists, especially in the reduction in alkali content from agricultural biomass and degradation of mill performance in the grinding of torrefied biomass. These challenges result in agglomeration, corrosion, and a reduction in combustion efficiency due to a higher percentage of unburned carbon in fly ash. Alternatively, HTC processing, where biomass is treated with hot compressed water instead of drying, reveals a key benefit, which is the focus of this work. It has been found that the alkali content of HTC biocarbon is reduced by 80% compared to that of raw miscanthus [17,18]. The biocarbon contained lignite-like characteristics and higher energy density, hydrophobicity, grindability, and pellet durability compared to dry torrefaction. Additionally, the biocarbon displayed better chemical and biochemical stability than its raw feedstocks. Using wet biomasses requires significantly less process water (PW) to obtain the desired dry weight content. For continuous operation, 20% of the PW may need to be removed from the system. Marija Mihajlović et al. [19] found that when miscanthus is hydrothermally carbonized at 220 °C for a 1 h residence period, ash content was reduced from 2.67% to 0.88%, while the higher heating value (HHV) increased from 18.35 to 21.18 MJ/kg. A study conducted by Aidan Mark Smith et al. [20] found that HTC biocarbon produced from miscanthus at 250 °C and 1 h residence period avoided slagging and fouling problems as the ash degradation temperature raised from 1040 °C to 1320 °C. However, a higher-severity processing condition (e.g., very high temperature and pressure) is required to increase the carbon content to similar levels as bituminous coal or pulverized coal injection (PCI) coal, which is a great operational challenge due to the process safety concerns related to high pressures.

Slow pyrolysis is another thermochemical process in which biomass undergoes chemical decomposition at elevated temperatures (above 430 °C) and in the absence of oxygen at atmospheric pressure. In general, pyrolysis of biomass will release some volatiles in the form of gases such as CO, CO₂, H₂, and CH₄ and will leave a solid residue enriched in carbon called pyro-biocarbon [21]. Biocarbon with a carbon content similar to PCI coal can easily be obtained by increasing the processing temperature. However, slow pyrolysis processing alone is not suitable for reducing ash and alkali matters because pyrolysis can even increase the ash content due to volatile matter (VM) loss. Pyrolysis occurs in three different steps. During the first step, moisture and some volatiles leave the biomass. In the second

step, primary pyro-biocarbon starts forming, and in the last step, primary pyro-biocarbon further decomposes at a slow rate, forming the carbon-rich solid [22]. Therefore, this process requires a higher amount of energy when wet biomass such as green agricultural crops or residues are used.

In this research, we propose a novel hybrid hydrothermal and slow pyrolysis process that is expected to have the synergistic benefits of both processes to produce biocarbon with low alkaline and phosphorous content, and with higher carbon content from agricultural biomass. Biomass ash content increases as a result of slow pyrolysis, so a lower ash content after hydrothermal carbonization will help to ensure the ash content remains low after pyrolysis. Additionally, the composition of biomass ash, specifically the fact that it is higher in Alkali compounds such as K_2O and Na_2O , which may cause slagging, makes ash content of higher concern in biomass-derived biocarbon compared to PCI coal. Therefore, it is necessary to reduce the ash content significantly before using in the blast furnace. Since the HTC process causes a significant reduction in ash yield by removing the inorganic elemental compositions in the liquid by-product, an optimized HTC condition is, therefore, necessary before slow pyrolysis. Firstly, the optimum condition for HTC at which the ash content is minimum should be found. At this stage, ash content would be minimized, and the carbon content of HTC biocarbon would be significantly greater than the initial content. This HTC biocarbon may then undergo pyrolysis to increase the carbon content further to the standards of the ironmaking process. In this study, miscanthus, which is one of the most common agricultural biomass residues, is considered to be a potential feed for ironmaking furnaces. As discussed, miscanthus firstly undergoes HTC to find the optimum condition at which the minimum ash content is obtained. Afterwards, the optimum HTC biocarbon undergoes slow pyrolysis at different operating conditions to enrich the carbon content to the desired value. The obtained product after HTC and slow pyrolysis will then be compared to the standard of the current PCI coal used in ironmaking furnaces. To characterize the biomass, HTC biocarbon, and pyro-biocarbon in different stages, proximate analysis, ultimate analysis, bomb calorimetry, thermogravimetric analysis (TGA), and Fourier-transform infrared spectroscopy (FTIR) experiments were performed. To the best of the authors' knowledge, no previous study has been performed to produce biocarbon from agricultural biomass by the combination of hydrothermal carbonization and pyrolysis processes for this purpose. The results obtained in this study can help the ironmaking industries to take an important step for reducing the environmental impacts of GHG emissions.

2. Materials and Methods

2.1. Raw Material

Miscanthus, which is one of the most common agricultural biomasses of Ontario, Canada, was used as the feedstock. The feedstock was obtained from a farm in Drumbo, Ontario and manually chopped into smaller pieces. Miscanthus, a purpose-grown energy crop, usually requires very little maintenance to produce and has a relatively high yield and energy content. Different methods of bioenergy production including hydrochar, biochar, biogas and bioethanol production have been investigated using miscanthus. The biowastes generated after those bioenergy production processes have been studied to use in the degraded and contaminated soils to improve the fertility of the soil [16]. The PCI coal sample was collected from the ArcelorMittal Dofasco G.P. steel manufacturing industry located in Hamilton, Ontario, Canada. A mill grinder (Model: Retsch PM-100) was then used to pulverize biomass and PCI coal samples into finer particles with a size less than $710\ \mu m$. The samples were then carefully stored in aluminum pans and then sealed with plastic bags.

2.2. HTC Experiments

A 780 W heater, a glass liner (762HC3), and a bench top mini Parr HTC reactor (600 mL series 4560) were used to perform the HTC experiments (Figure 1).

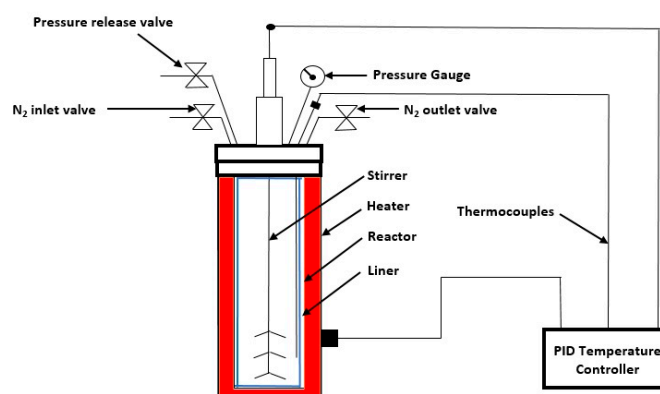


Figure 1. Schematics of the lab-scale experimental set up of the HTC process.

The pressure during the experiment was monitored with a pressure gauge fitted at the top of the reactor. For controlling the temperature of the process, a PID temperature controller was used. To evaluate the impact of different operating conditions during the hydrothermal carbonization process, the experiments were performed at various operating temperatures and residence times (15, 30 and 45 min) suggested by the Design Expert 11 software. Firstly, around 10 g of as-received biomass samples were placed in the glass liner and mixed with deionized water at approximately a 1:12 biomass water ratio. The liner was inserted, and the HTC reactor was closed with the reactor head by the bolts. To create an air-free environment inside the reactor, it was purged 5–6 times by the nitrogen gas prior to the reaction. The reactor was then pressurized to 1.5–2.0 MPa (absolute) to ensure the pressure in the reactor was maintained higher than the water saturation pressure. The heater was then used to heat the reactor. A thermocouple was placed inside the reactor, which was coupled with the data-logger to record the temperature of the biomass-water mixture. When the internal temperature reached the desired HTC temperature, the stopwatch was started, and the reactor temperature was maintained within ± 5 °C for the duration of the experiment.

After the fixed residence time, the reactor was quickly submerged into ice water to dramatically decrease the temperature of the reactor within 5–7 min. Once cooled, the gaseous product produced during the process was released into a hood by the pressure release valve. Filter papers with a pore diameter of 20 μm were used to separate the HTC biocarbon and the process water. A muffle furnace (F48055-60) at 105 °C was used to remove the moisture content from the HTC biocarbon. The samples were dried overnight. To ensure consistency and reproducibility, each experiment was repeated three times. The dried HTC biocarbon sample was then weighted, and the following equations were used to determine their respective process parameters:

$$\text{Mass Yield} = \frac{\text{Mass of dried HTC/Pyro biocarbon}}{\text{Mass of dried Raw biomass}} \times 100 \quad (1)$$

$$\text{Energy Densification Ratio} = \frac{\text{Higher Heating Value of HTC/Pyro biocarbon}}{\text{Higher Heating Value of Raw Biomass}} \quad (2)$$

$$\text{Energy Yield} = \text{Mass Yield} \times \text{Energy Density Ratio} \quad (3)$$

2.3. Slow Pyrolysis

For the slow pyrolysis experiment, a macro TGA reactor was used. The reactor was prepared and calibrated at the University of Guelph (Figure 2). The reactor consisted of a stainless-steel tube of 175 mm height and 15 mm diameter. The hydrothermally pretreated HTC biocarbon samples were weighed before slow pyrolysis. The reactor was then connected to a nitrogen cylinder by the nitrogen inlet line above the reactor head. Two ball valves were set on the inlet line to control nitrogen flow from the high-pressure nitrogen cylinder to low pressure reactor cavity. During the experiment, a 5 mL/min

flow of nitrogen gas was constantly maintained to ensure an inert atmosphere in the reactor chamber. A flow meter was set in the nitrogen inlet line after the ball valves to continuously monitor the nitrogen flow rate from the cylinder during the process. The reactor after purging with nitrogen was then inserted inside a Muffle Furnace (Model F48055-60, USA) to heat up the pyrolysis reactor. The reactor was subjected to a heating rate of 15 °C/min to reach 3 different temperatures (350, 400, 450 °C). A k-type thermocouple was used to continuously record the core temperature of the bio-carbon sample. The k-type thermocouple was connected to a data-logger to continuously visualize and record the temperature profile. A stopwatch was used to countdown retention times (15, 30 and 45 min) after the reactor reached the desired setpoint temperature. The outlet line fitted to the reactor head was used to drive out the nitrogen gas and other produced gases during the pyrolysis process. The outlet line was inserted inside a water bath to prevent direct emission of the process gas into the environment. The water bath temperature was maintained around 0–5 °C to condense the condensable gases produced during the process. The water bath was placed below a fume hood so that no non-condensable gases (toxic and non-toxic) could contaminate the lab environment. The furnace was immediately shut down after the retention time to cool down the reactor. The nitrogen flow continued at the same flow rate until the pyrolyzed samples were taken out. As soon as the reactor temperature dropped to room temperature, the pyrolyzed samples were taken out of the reactor and weighed again. Each experiment was carried out in triplicate to ensure the consistency and reproducibility of the research.

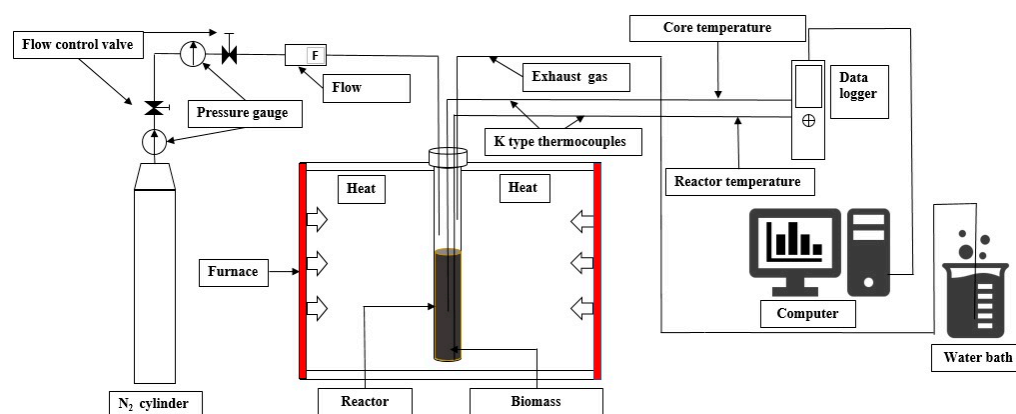


Figure 2. Schematics of the lab-scale experimental set up of the slow pyrolysis process.

2.4. Characterization Tests

2.4.1. Higher Heating Value (HHV)

The HHV of raw biomass, pyrolyzed biomass, and HTC pretreated biomass samples were measured by using an IKA-C200 bomb calorimeter. Between 0.5 and 1 g of the samples were filled into the crucible before putting the crucible inside the vessel. Before putting the vessel into water, it was closed tightly and pressurized with pure oxygen to 3000 KPa to ensure that enough oxygen was available in the vessel for combustion. Ignition was created inside the vessel by a cotton thread hinged from the vessel circuit wire to the sample surface, which in turn resulted in the combustion of the sample. The heat generated inside the vessel due to combustion was transmitted to the water for measurement. The HHV of the sample was calculated by using the temperature difference of water before and after the heating by the following equation:

$$HHV = \frac{C \times \Delta T - Q_e}{M} \quad (4)$$

where M = the sample weight,

C = the bomb calorimeter's heat capacity,

ΔT = Temperature deviation of the heated and cold water, and

Q_e = Heat generation due to thread ignition

2.4.2. Thermogravimetric Analysis

A micro-TGA SDT Q 600 machine was used to perform the TGA analysis of the raw and HTC biocarbon, and pyro-biocarbon samples. The samples were dried overnight prior to being used for thermo-gravimetric analysis. Two platinum crucibles were used for this process, one crucible as a balance and another one for holding the samples. Samples of around 10 mg were put into the crucible for the analysis. The furnace was then heated at a heating rate of 20 °C/min, and the inner temperature of the furnace increased from 25 °C to 1000 °C. A continuous 50 mL/min air flow rate was maintained inside the furnace, ensuring higher air flow rate than the amount of stoichiometric air [23]. The weight losses shown represent the combustion phenomenon taking place. To plot the DSC-TGA plots, Thermal Analysis Universal software 2000 was used.

2.4.3. Ultimate Analysis

For performing the elemental analysis of the raw and HTC biocarbon, and pyro-biocarbon specimens, a Flash 2000 Elemental Analyzer was used. Around 2.0 ± 0.5 mg dry samples were placed in tin crucibles for elemental analysis. Afterwards, the crucibles were sealed carefully and then placed into the sample tray of the analyzer. The elemental analyzer analyzed the percentage of carbon, nitrogen, hydrogen, and sulfur contents and the amount of oxygen content was estimated by the following equation [24]:

$$O\% = 100\% - (C\% + H\% + N\% + S\% + Ash\%) \quad (5)$$

2.4.4. Proximate Analysis

A muffle furnace was used to perform the proximate analysis to determine the volatile matter, ash content, and moisture content of the raw sample, HTC biocarbon, and pyro-biocarbon. ASTM E1756 followed to measure the moisture content of the samples where a porcelain crucible containing 0.5–1.0 g of samples was put inside the furnace for 24 h at 105 °C. The samples were then cooled in a desiccator. The weight loss of the samples before and after the experiment represents the moisture content. For measuring the ash content, this was followed by ASTM E1755, where a porcelain crucible with 0.5–1.0 g of sample was burned for 5 h at 575 °C and the weight difference of the sample was used to determine the ash content in it. In accordance with ASTM E872, the volatile matter was estimated, whereby 0.5–1.0 g of sample was put in a platinum crucible and after covering the platinum crucible with a platinum cover, it was kept in the furnace at 950 °C for 7 min. The difference in weight before and after the process showed the volatile matter content in the sample. Subtracting the volatile matter, moisture content, and ash content from 100%, the fixed carbon content for each sample was determined [25].

2.4.5. Fourier-Transform Infrared Spectroscopy (FTIR)

An FTIR spectrometer was used to analyze the gases leaving the reactor during the combustion of the milled oven-dried raw sample, HTC biocarbon, and pyro-biocarbon samples in 400–4000 cm^{-1} wave number range. Liquid nitrogen in the IR instrument Varian 660-IR was used to cool down the MCTA detector. The machine collected the spectra at 4 cm^{-1} resolutions.

2.5. The Standard Feed Characteristics for Ironmaking Furnaces

The main goal of this research was to find a renewable alternative for the PCI coal used in the BF. The criteria for such an alternative were determined based on the characteristics of the PCI coal currently used in the BF ironmaking process. As seen in Table 1, the carbon content, fixed carbon (FC) composition, and HHV were significantly lower in the raw miscanthus than in the PCI coal, whereas the oxygen content and volatile matter (VM) content were much higher. This indicates that raw miscanthus is too dissimilar from PCI

coal in terms of physiochemical properties. The ash content of raw miscanthus is lower than that of PCI coal, which is one desirable trait. As such, to use miscanthus in ironmaking furnaces as a replacement for PCI coal, significant changes to the physiochemical properties must be made.

Table 1. Physicochemical properties of PCI coal and raw miscanthus.

Properties	PCI Coal	Raw Miscanthus
C(%)	77.66 ± 1.45	46.43 ± 1.1
H(%)	4.1 ± 0.62	5.8 ± 0.7
N(%)	1.76 ± 0.29	0.16 ± 0.03
S(%)	0.3 ± 0.07	0
O(%)	9.53 ± 1.3	45.53 ± 0.57
Ash(%)	6.65 ± 1.1	2.08 ± 0.2
FC(%)	56.94 ± 1.84	10.28 ± 1.15
VM(%)	36.41 ± 0.82	87.64 ± 1.91
HHV(MJ/Kg)	32.07 ± 0.67	18.06 ± 0.38

2.6. Response Surface Methodology

Due to the high number of required experiments, and the need for optimization of some of the parameters, especially the ash content, the response surface methodology (RSM) was used. RSM explores the relationship of the explanatory variables and the desired response variables by designing a set of experiments and finding the optimal response [13]. In this study, RSM was used to find the relations of time and temperature of HTC with different responses, including the ash content. The range of the variables of the experimental design are given by Table 2, and the responses and their units are reported in Table 3.

Table 2. Range of the variables for the experimental design.

Factor	Name	Units	Type	Minimum	Maximum
A	Temperature	°C	Numeric	190.00	220.00
B	Time	min	Numeric	15.00	45.00

Table 3. Response factors and respective units.

Name	Units	Type	Low	High
C	wt%	Response	47.8	60.41
H	wt%	Response	5.37	8.86
N	wt%	Response	0	0.16
O	wt%	Response	33.86	45.73
Ash	wt%	Response	0.19	0.69
VM	wt%	Response	71.74	87.2
Fixed Carbon	wt%	Response	12.14	28.02
HHV	Mj/Kg	Response	18.5	23.64
Mass Yield	wt%	Response	57.09	75.55
Energy Yield	wt%	Response	70.4096	77.963

Based on Tables 3 and 4, a flexible design structure (combined, and user defined) was performed to find a custom model for the HTC of miscanthus. A total run of 16 experiments for HTC was designed by Design-Expert 11 (Stat-Ease, Inc., Minneapolis, MN, USA) in randomized order and the output responses were entered from HTC experiments. The maximum and minimum values for the HTC operating temperature and residence time to find the optimum operating condition were selected from the literature [17]. The table of the designed experiment conditions, the responses, and the analysis of the optimization in Design-Expert are given in the Results and Discussion section.

Table 4. HTC and characterization results of the designed experiments in Design-Expert.

	Factor 1	Factor 2	Response 1	Response 2	Response 3	Response 4	Response 5	Response 6	Response 7	Response 8	Response 9	Response 10
Run	A:Temperature	B:Time	C	H	N	O	Ash	VM	Fixed Carbon	HHV	Mass Yield	Energy Yield
	°C	min	wt%	wt%	wt%	wt%	wt%	wt%	wt%	Mj/Kg	wt%	wt%
1	205	30	53.33	5.76	0	40.67	0.24	82.84	16.92	21.08	63.9	72.8115
2	220	15	55.2	5.72	0.12	38.72	0.24	79.65	20.11	21.94	59.37	70.4096
3	190	45	52.87	5.84	0.11	40.49	0.69	83.77	15.54	20.34	66.18	72.7622
4	205	15	52.4	5.86	0.11	41.38	0.25	84.16	15.59	20.42	66.14	73.0043
5	205	45	54.41	5.7	0.14	39.53	0.22	81.99	17.79	21.44	62.98	72.9887
6	190	30	51.6	8.86	0.1	39.24	0.2	85.23	14.57	20.3	71.05	77.963
7	205	30	53.35	5.81	0	40.63	0.21	82.88	16.91	21.1	63.91	72.8919
8	190	15	47.8	5.65	0.16	45.73	0.66	87.2	12.14	18.5	75.55	75.55
9	220	45	60.41	5.37	0.12	33.86	0.24	71.74	28.02	23.64	57.09	72.9518
10	220	30	57.45	5.55	0.1	36.65	0.25	76.77	22.98	22.75	57.56	70.7832

3. Results and Discussion

3.1. Ultimate, Proximate and HHV Analysis of the HTC Experiments

The results of the 10 HTC experiments and characterization of the obtained HTC biocarbon samples are reported in Table 4. Mean and standard deviation of the results are given in Table 5.

Table 5. Mean and Std. Dev of results.

Name	Units	Minimum	Maximum	Mean	Std. Dev.	Model
C	wt%	47.8	60.41	53.31	3.50	Linear
H	wt%	5.37	8.86	5.89	0.8005	Quadratic
N	wt%	0	0.16	0.0944	0.0597	Quadratic
S	wt%	0	0	0.0000	0.0000	No model chosen
O	wt%	33.86	45.73	40.36	3.28	No model chosen
Ash	wt%	0.19	0.69	0.3381	0.1988	Quadratic
VM	wt%	71.74	87.2	82.16	4.20	Quadratic
Fixed Carbon	wt%	12.14	28.02	17.50	4.31	Quadratic
HHV	Mj/Kg	18.5	23.64	20.93	1.48	Linear
Mass Yield		57.09	75.55	65.19	6.28	2FI
Energy Yield		70.4096	77.963	73.31	2.09	2FI

With increased operating time and temperature, the mass yield decreased. Similar results have been found in the literature [17–19,26]. The effect of the reaction time was not observed to be as prominent as the effect of reaction temperature. The mass yield decreased from 75.55% to 59.37% with a 30 °C increase in the reaction temperature from 190 °C to 220 °C with a 15-min residence time. Similarly, with the increase in the reaction temperature from 190 °C to 220 °C for 30 and 45 min, the mass yield decreased from 71.05% to 57.56% and from 66.18% to 57.09%, respectively. HHV of HTC biocarbon samples increased with increasing operating temperature and residence time.

3.2. Optimization of HTC with Respect to Minimum Ash

Although HTC can improve the carbon content and HHV of the biomass, the main purpose of using HTC in this study was to minimize the ash content. Using the Design-Expert software, an adequate relationship between the HTC variables (temperature and time) and all responses can be developed. A quadratic polynomial equation was suggested by the software due to its higher accordance with the experimental results when compared with other equations. The equation in terms of actual factors is shown in Equation (1). The Adjusted R² of 0.98 showed the high accuracy of the model.

$$\text{Ash} = 30.84221 - 0.283019 T - 0.042386 t + 0.000064 Tt + 0.000662 T^2 + 0.000458 t^2 \quad (6)$$

where T and t represent operating temperature and time, respectively.

Using the response surface methodology, the effects of time and temperature on the ash content were found, as shown in Figure 3 and Equation (6). As can be seen, both temperature and time have a negative correlation with the ash content. Temperature has a higher negative effect on the ash content with a coefficient of -0.28 , which is in agreement with the literature [17,27]. Moreover, the interaction between temperature and time is negligible. The ash content hits the minimum at a few points, including 199 °C, 28 min. Hence, considering the severity of the HTC process, 199 °C and 28 min was selected as the optimum point for the application of ironmaking process.

Design-Expert® Software

Factor Coding: Actual

Ash (Wt%)

● Design points above predicted value

○ Design points below predicted value

0.19 0.69

X1 = A: Temperature

X2 = B: Time

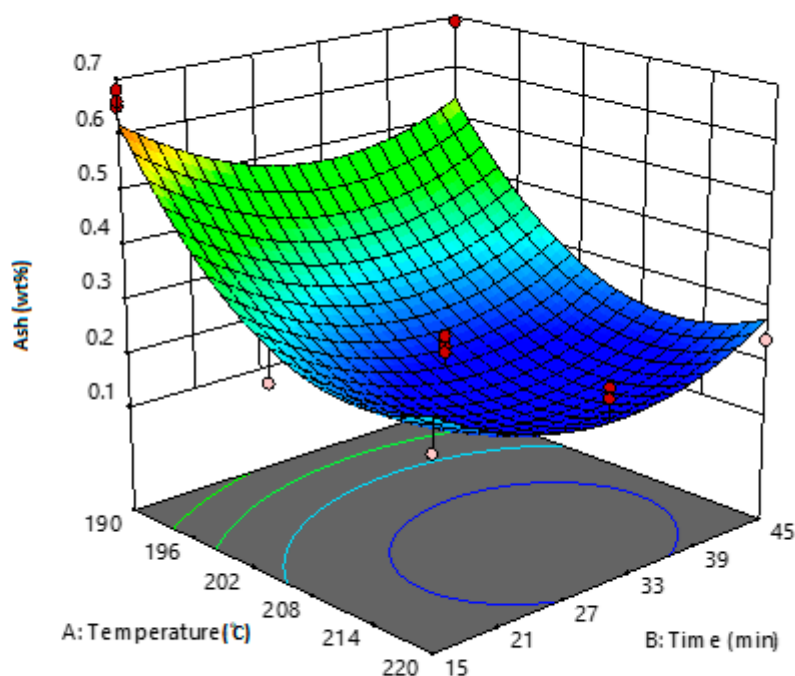


Figure 3. 3D response surface plot of the ash content considering the interactions of temperature and time.

To validate the overall models developed by the RSM, the optimized solution (199 °C and 28 min) was tested experimentally using the same methodology explained for the previous HTC tests. A comparison of the experimental results with the values obtained from the model at this condition showed that the percentage error was never higher than 1%. Therefore, the accuracy of the optimum model was validated.

3.3. Effect of HTC and Slow Pyrolysis Pretreatment Condition on Fuel Properties

Table 3 shows that the lowest ash content HTC biocarbon was obtained under HTC-199-28 operating conditions. However, in the Van-Krevelen diagram, the position of this HTC biocarbon fuel is within the biomass range, meaning it is not a suitable fuel for co-firing with the coal. As such, slow pyrolysis of the HTC-199-28 samples was performed to produce pyro-biocarbon with an equivalent fuel quality to coal, but with less ash content than if slow pyrolysis alone had been performed. The HTC-199-28 samples were thus slow pyrolyzed for eight different operating conditions. Table 6 presents the proximate analysis of the pyro-biocarbon produced by the slow pyrolysis of HTC-199-28 HTC biocarbon samples under eight different operating conditions. The slow pyrolysis process significantly reduced the volatile matter from the feedstock, although it was not able to reduce the ash content due to the higher devolatilization temperature of the ash, forming inorganic elements. It can be seen that while the optimized HTC process alone did not alter the physiochemical properties enough to match PCI coal, the slow pyrolysis caused a significant change in the key properties, including increasing fixed carbon content, HHV, and slightly increasing ash, while decreasing volatile matter content. Comparing the SP-400-30 sample and PCI coal, the SP-400-30 sample has higher fixed carbon content and HHV, while maintaining substantially lower ash content relative to PCI coal. As such, this process is the lowest-severity process that can mimic the properties of PCI coal from miscanthus biomass.

Table 6. Proximate analysis of the optimized HTC biocarbon and slow pyrolysis-derived pyro-biocarbon samples.

Sample Name	Volatile Matter (%)	Ash Content (%)	Fixed Carbon	HHV(MJ/Kg)	Mass Yield (%)
Raw miscanthus	87.64 ± 1.91	2.08 ± 0.2	10.28 ± 1.15	18.06 ± 0.38	-
HTC-199-28	84.66 ± 1.37	0.24 ± 0.07	15.1 ± 1.77	20.37 ± 1.15	66.97 ± 2.12
SP-350-30	44.76 ± 0.35	0.65 ± 0.19	54.59 ± 2.1	30.67 ± 1.89	39.77 ± 1.55
SP-350-45	43.08 ± 0.55	0.71 ± 0.22	56.21 ± 1.4	31.85 ± 1.44	38.23 ± 1.18
SP-400-15	36.85 ± 0.28	0.72 ± 0.12	62.43 ± 1.95	31.49 ± 2.12	31.56 ± 2.34
SP-400-30	35.5 ± 0.52	0.79 ± 0.13	63.71 ± 2.45	32.59 ± 1.92	30.59 ± 1.37
SP-400-45	33.97 ± 0.23	0.85 ± 0.14	65.18 ± 1.85	32.97 ± 1.16	29.84 ± 1.85
SP-450-15	24.9 ± 0.18	0.95 ± 0.23	74.15 ± 1.38	31.69 ± 1.84	29.76 ± 1.69
SP-450-30	23.4 ± 0.39	0.99 ± 0.37	75.61 ± 1.14	33.1 ± 1.18	27.92 ± 2.05
SP-450-45	23.3 ± 0.29	1.01 ± 0.26	75.69 ± 1.62	33.4 ± 1.35	26.65 ± 1.35
PCI coal	36.41 ± 0.82	6.65 ± 1.1	56.94 ± 1.84	32.07 ± 0.67	-

Slow pyrolysis significantly increased the carbon content of the HTC biocarbon sample while sharply reducing its oxygen content. The HTC process significantly reduced the ash content from raw miscanthus samples. The main limitation of the HTC process is that it cannot significantly increase the carbon content into the HTC biocarbon at low–moderate operating temperatures. At high operating temperatures, the pressure inside the reactor rises higher, which creates safety concerns during the process operation. Additionally, at higher temperatures, the alkali and alkaline earth metal levels were higher than at the moderate HTC reaction temperature, which is supported in the literature [18]. With the increase in reaction severity, the atomic O:C ratio decreased sharply. This decreasing trend exhibited increasing fuel combustion and heating characteristics from the Van-Krevelen diagram perspective.

Although the slow pyrolysis process significantly reduced the oxygen content and increased the carbon content of the pyro-biocarbon, it did not significantly change the hydrogen or nitrogen content. A slight increase in the ash content was also observed after the slow pyrolysis process. At slow pyrolysis of 400 °C for 30 min, the ash content increased to 0.79%, while it was only 0.24% for the HTC-199-28 HTC biocarbon sample.

Since the reaction kinetics have still not been fully addressed for slow pyrolysis, the reason for the increase in alkali and alkaline matter with increasing reaction severity is not yet known. Although the pyro-biocarbon produced at 400 °C and 30 min had higher ash content than the HTC biocarbon sample, it was still lower than the ash content of the pulverized coal used in the ironmaking process, as shown in Table 7.

Table 7. Comparison of the physicochemical properties of selected pyro-biocarbon and PCI coal.

Properties	SP-400-30	PCI Coal
C(%)	79.67 ± 1.62	77.66 ± 1.45
H(%)	4.5 ± 0.75	4.1 ± 0.62
N(%)	0.35 ± 0.08	1.76 ± 0.29
S(%)	0	0.3 ± 0.07
O(%)	14.69 ± 1.7	9.53 ± 1.3
Ash(%)	0.79 ± 0.13	6.65 ± 1.1
FC(%)	63.71 ± 2.45	56.94 ± 1.84
VM(%)	35.5 ± 0.52	36.41 ± 0.82
HHV(MJ/Kg)	32.59 ± 1.92	32.07 ± 0.67

The atomic H/C and O/C ratios of raw and HTC pretreated miscanthus samples are displayed in Figure 4 using a Van-Krevelen diagram. It is clear that raw miscanthus has low carbon and high oxygen content relative to the pulverized coal used in energy-intensive industrial applications. The HTC biocarbon produced at low–moderate temperatures showed almost the same fuel properties as biomass. Since the HTC process alone is not promising enough to simultaneously release the highest amount of alkali and alkaline

matter, maximize the carbon content, and minimize the oxygen content, a hybrid HTC and slow pyrolysis process could be an effective pathway for finding higher-fuel-quality pyro-biocarbon with minimal ash content.

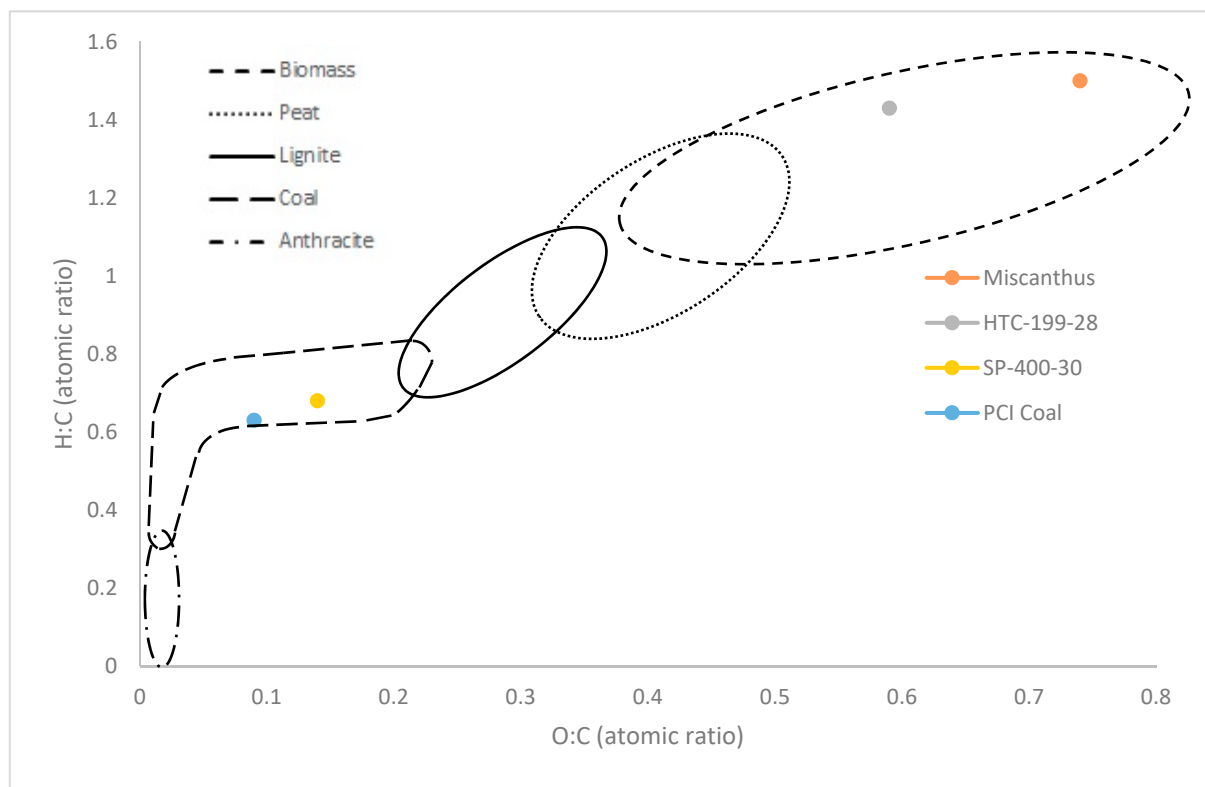


Figure 4. Van-Krevelen diagram showing different atomic O:C and H:C ratios of different samples.

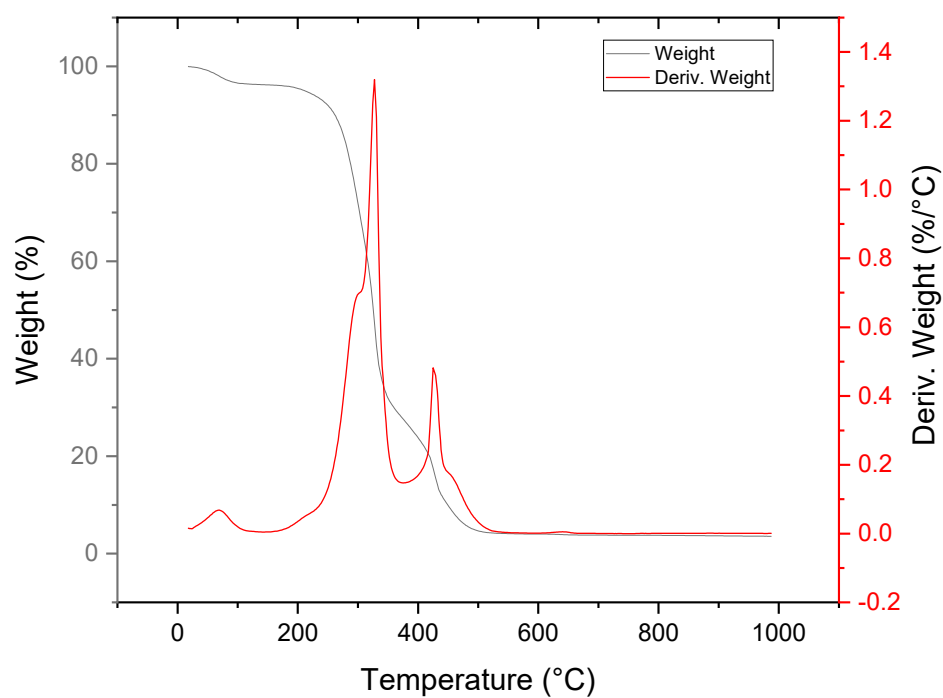
Slow pyrolysis can significantly increase the carbon content of the HTC biocarbon sample and the oxygen content decreased dramatically. While the HTC-199-28 sample was in the biomass region of the Van-Krevelen diagram, the slow pyrolysis upgraded them into bituminous coal without significantly increasing the ash content. The SP-400-30 sample exhibited similar fuel characteristics to those of the pulverized coal samples, as shown in Table 7.

3.4. Effect on the Thermal Degradation and Combustion Characteristics

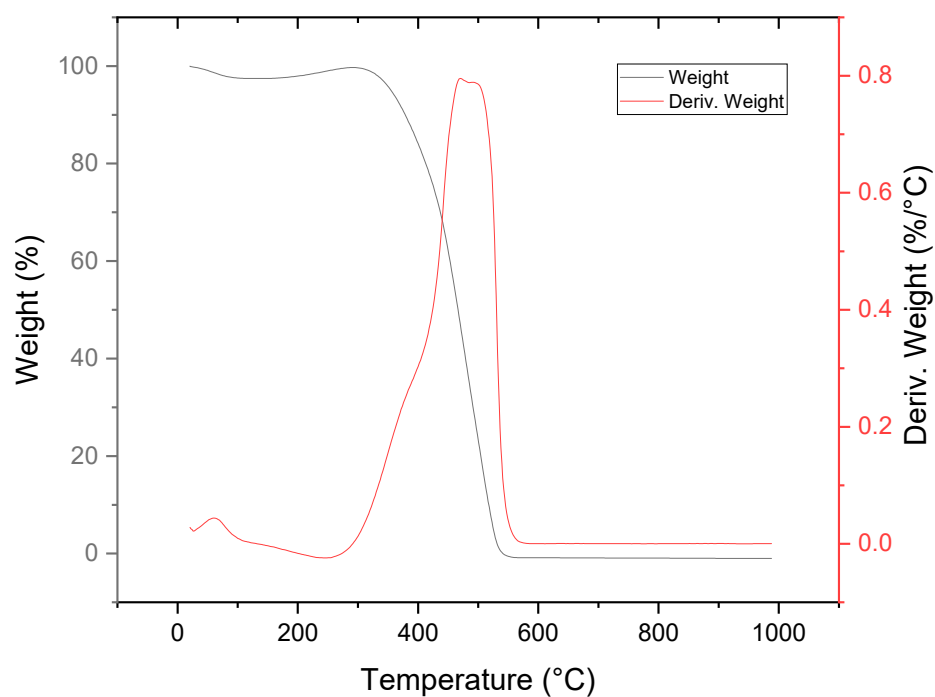
Figure 5 represents the TGA/DTG graphs of raw miscanthus, SP-400-30 pyro-biocarbon, and PCI coal samples, respectively.

For raw miscanthus, approximately 10% weight loss occurred at about 100 °C due to the evaporation of the moisture content from the biomass. Approximately 60% weight loss occurred between 280 and 320 °C due to the thermal degradation of hemicellulose and cellulose contents. The lignin was decomposed by heating at around 450 °C [28]. Since the pyro-biocarbon sample was not analyzed immediately after drying, the weight loss due to the moisture release was more substantial than that of the raw sample. Since the HTC process significantly decomposed the hemicellulose content, the sample became richer in cellulose and lignin, and its thermal stability was improved. For the pyro-biocarbon samples, the hemicellulose and cellulose content was completely decomposed after being subjected to the inert thermal carbonization process. Thus, the large weight loss observed for all the pyro-biocarbon samples was for the decomposition of lignin. The decomposition due to the thermal degradation of lignin occurred at approximately 500 °C for the biocarbon sample [28]. Comparing these results with the TGA/DTG curve for PCI coal shows that the curve for the pyro-biocarbon samples was more similar to the PCI coal curves. Despite

this, the peak degradation temperature for the pyro-biocarbon at 500 °C was still lower than the 600 °C peak for the PCI coal sample.



(a)



(b)

Figure 5. Cont.

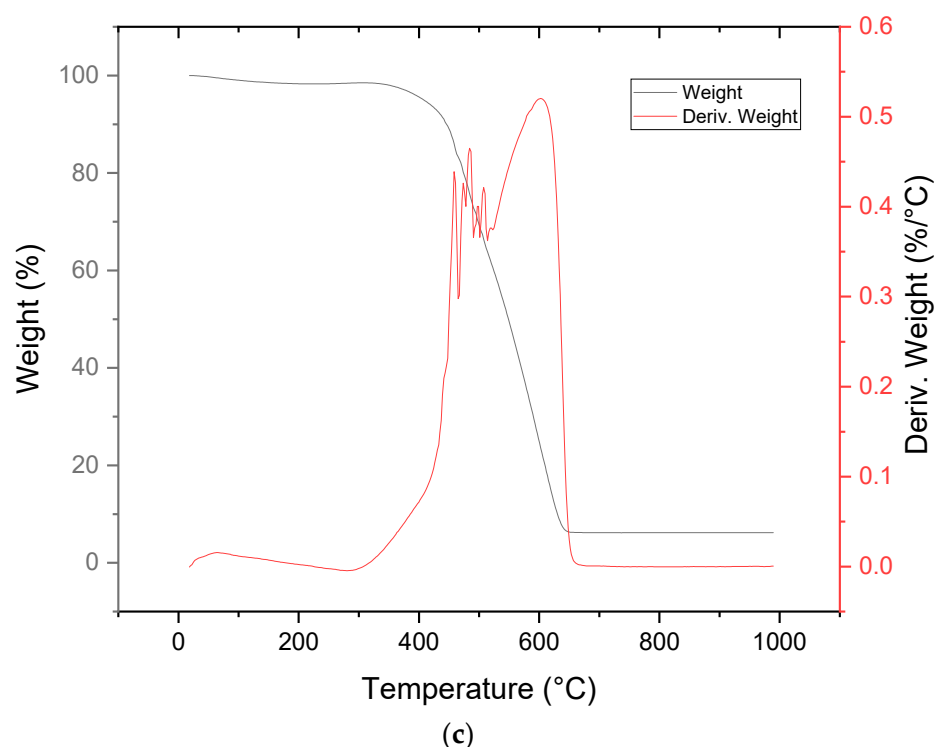
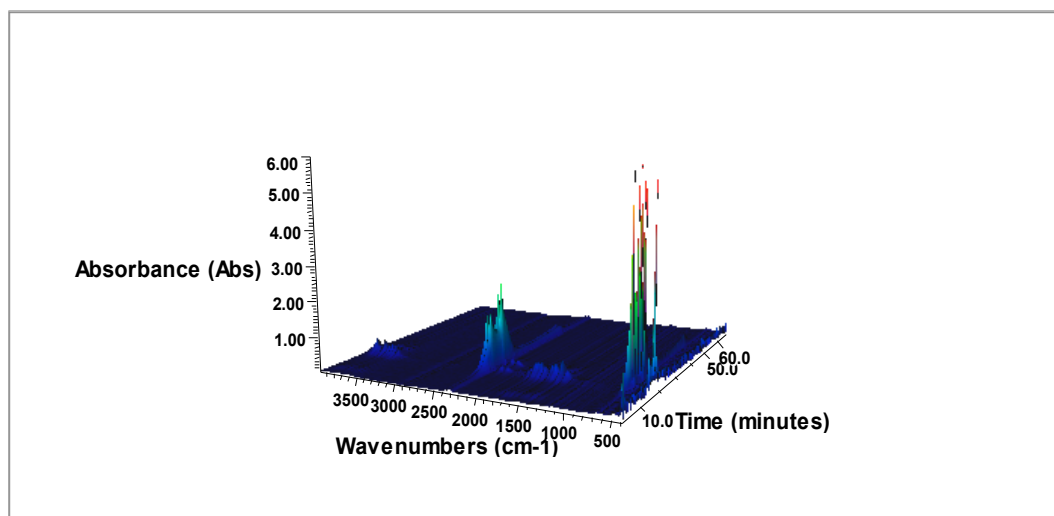
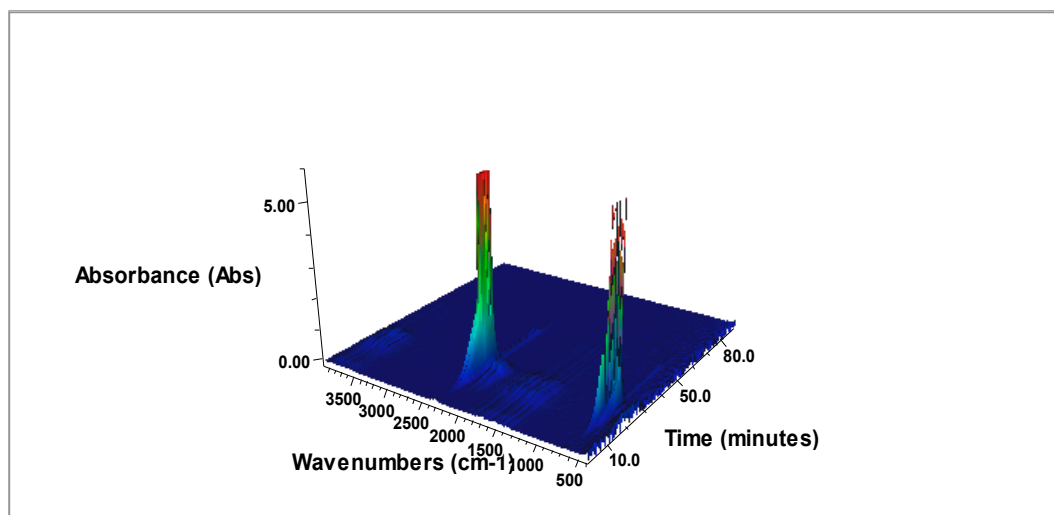


Figure 5. TGA/DTG graphs for (a) raw miscanthus, (b) SP-400-30, (c) PCI coal.

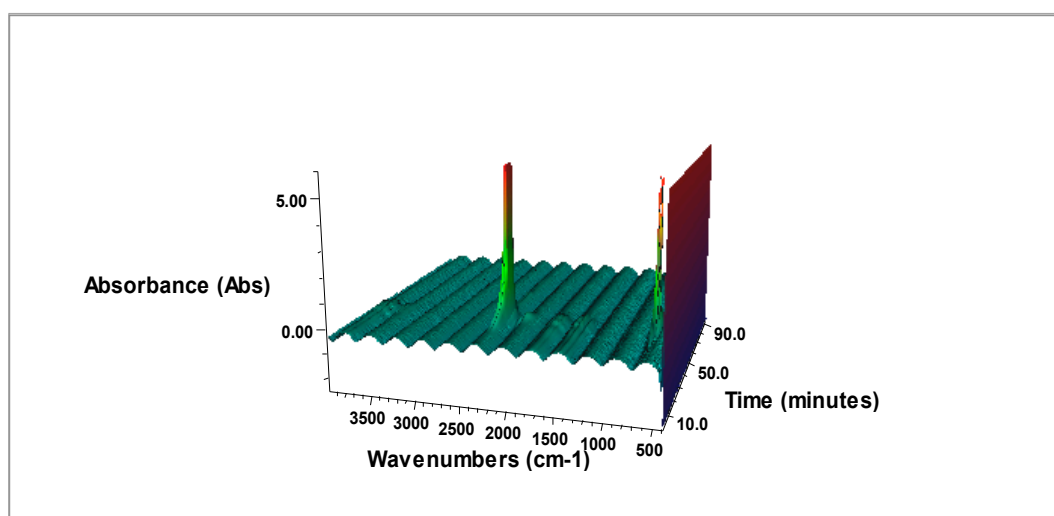
Figure 6 shows the 3D FTIR images with respect to wavenumber, absorbance, and time for the raw miscanthus, pyro-biocarbon and PCI coal samples, respectively. The main peaks observed in the figure are mainly between $2402\text{--}2240\text{ cm}^{-1}$ and $736\text{--}605\text{ cm}^{-1}$, showing the release of CO_2 and CO , respectively, during the combustion process, indicating the presence of C=O bonding. The peaks at wavenumber $2402\text{--}2240$ are much more prevalent in the pyro-biocarbon and PCI samples relative to the raw sample; however, the raw sample contains additional peaks. For the raw sample, a weak stretch in the $4000\text{--}3500$ wavenumber region indicates the presence of OH groups, and vibrations in the $1650\text{--}1450$ wavenumber region are indicative of C=C aromatic rings. These peaks are no longer visible in the pyro-biocarbon sample, as the high-temperature thermal treatment removes some of the functional groupings. Since the samples were oven dried prior to FTIR analysis, the release of water vapor was not observed.



(a)



(b)



(c)

Figure 6. FTIR images showing release of combustion gases leaving (a) raw miscanthus, (b) SP-400-30, (c) PCI coal.

4. Conclusions

The increasing global concern regarding climate change resulting from GHG emissions from energy-intensive industries can be significantly addressed by partially substituting coal with biocarbon from biomass. For technically sustainable implementation of biocarbon in an environmentally and economically efficient manner, biocarbon needs to be suitable enough in terms of its combustion properties, emissions, and availability. The biocarbon needs to be a potential replacement for coal without further modification of the energy storage and transportation system. The hybrid HTC and slow pyrolysis process has emerged as an effective pretreatment for the conversion of high-ash-content biomass to low-ash pyro-biocarbon to produce a potential replacement for coal in ironmaking BF. The HTC process can significantly reduce the undesired alkali and alkaline matter from the fuel, which can significantly increase the combustion efficiency and the boiler safety. The slow pyrolysis step can then significantly increase the carbon content of the HTC biocarbon to increase the carbon content to coal-like levels. The pyro-biocarbon (SP-400-30) produced by slow pyrolysis of the HTC-199-28 sample exhibited the most similar combustion, emission, and fuel properties to the pulverized coal injection. It had a carbon content of 79.67%, which is higher than the PCI coal sample (77.66%). It also contained less ash (0.79%) than the PCI coal (6.65%). Therefore, it can be stated that using a hybrid hydrothermal and slow pyrolysis process, a cleaner renewable biofuel can be obtained from agricultural biomass. Assessment of Business Case for Purpose-Grown Biomass in Ontario (2012) stated that, at that time, there was approximately 500 acres of Miscanthus production in Ontario. However, it also stated that Miscanthus produces yields of 6–12 tonne/acre, the highest-yielding purpose-grown crop for combustion usage [29]. As such, a large amount of SP biocarbon would be able to be theoretically produced. However, the amount of replaceable coal would depend on the biocarbon performance during BF ironmaking, which is unable to be determined without testing as the performance may be highly sensitive to variations in composition (such as the higher oxygen content) or even carbon microstructure/porosity. That might be a potential future work in this research. Production of coke from coal involves heating the coal in the absence of oxygen to high temperatures to remove volatiles, very similar to pyrolysis. Therefore, the pyrolysis process should be technically feasible on large scales or be incorporated into existing large-scale upgrading processes. However, hydrothermal carbonization, due to the high pressure and temperature requirements, is not used in any large-scale operations, and as such would be difficult to directly implement with existing processes. Further in-depth research is necessary to critically investigate the effective use of HTC and slow pyrolysis processes for successful process design and simulation, as well as the performance of the pyro-biocarbon in a blast furnace environment. In addition, further studies need to be performed to evaluate the potential of this hybrid hydrothermal and slow pyrolysis process to produce biocarbon from a mixture of different types of residual biomass. Moreover, life cycle assessment (LCA) to determine the economic feasibility of this biocarbon production process might be a prospective future work.

Author Contributions: Conceptualization, T.D.A. and A.D.; methodology, T.D.A.; software, T.D.A.; validation, T.D.A., O.N. and M.H.; formal analysis, T.D.A.; investigation, S.T.; resources, T.D.A.; data curation, T.D.A.; writing—original draft preparation, T.D.A.; writing—review and editing, K.M.-W.; visualization, O.N.; supervision, A.D.; project administration, A.D.; funding acquisition, A.D. All authors have read and agreed to the published version of the manuscript.

Funding: This research was funded by Ontario Ministry of Agriculture, Food and Rural Affairs (OMAFRA).

Acknowledgments: The authors would like to acknowledge the research grants from Natural Sciences and Engineering Research Council of Canada (NSERC) Ontario Ministry of Agriculture, Food and Rural Affairs (OMAFRA), and Ministry of the Environment and Climate Change (MOECC) for Best in Science program. Financial support through the Biomass Canada Cluster (BMC) which is funded through Agriculture and Agri-Food Canada's AgriScience program and industry partners is also acknowledged.

Conflicts of Interest: The authors declare no conflict of interest.

References

- World Steel Association. *Steel Statistical Yearbook 2017*; World Steel Association: Brussels, Belgium, 2017.
- Mousa, E.; Wang, C.; Riesbeck, J.; Larsson, M. Biomass applications in iron and steel industry: An overview of challenges and opportunities. *Renew. Sustain. Energy Rev.* **2016**, *65*, 1247–1266. [\[CrossRef\]](#)
- Suopajarvi, H.; Pongrácz, E.; Fabritius, T. The potential of using biomass-based reducing agents in the blast furnace: A review of thermochemical conversion technologies and assessments related to sustainability. *Renew. Sustain. Energy Rev.* **2013**, *25*, 511–528. [\[CrossRef\]](#)
- Pardo, N.; Moya, J.A. Prospective scenarios on energy efficiency and CO₂ emissions in the European Iron & Steel industry. *Energy* **2013**, *54*, 113–128. [\[CrossRef\]](#)
- Birat, J. *Global Technology Roadmap for CCS in Industry Steel Sectoral Report Steel Sectoral Report Contribution to the UNIDO Roadmap on CCS 1-Fifth Draft*; United Nations Industrial Development Organization: Vienna, Austria, 2010.
- Sriram, N.; Shahidepour, M. Renewable biomass energy. In Proceedings of the IEEE Power Engineering Society General Meeting, San Francisco, CA, USA, 6 June 2005; pp. 1910–1915.
- Ng, K.W.; Giroux, L.; Todoschuk, T.; Wing, K.; Giroux, L.; Todoschuk, T. Value-in-use of biocarbon fuel for direct injection in blast furnace ironmaking. *Ironmak. Steelmak.* **2018**, *45*, 406–411. [\[CrossRef\]](#)
- Ng, K.W.; Giroux, L.; Macphee, T. Wood pellets for ironmaking from a life cycle analysis perspective. In Proceedings of the AISTech—Iron and Steel Technology Conference Proceedings, Atlanta, GA, USA, 7–10 May 2012; pp. 331–338.
- Ng, K.W.; Giroux, L.; Todoschuk, T. *Reduction in GHG Emission of Steel Production by Direct Injection of Renewable Biocarbon*; Springer: Copenhagen, Denmark, 2018; pp. 903–912. [\[CrossRef\]](#)
- Nidheesh, P.V.; Kumar, M.S. An overview of environmental sustainability in cement and steel production. *J. Clean. Prod.* **2019**, *231*, 856–871. [\[CrossRef\]](#)
- Mäkelä, M.; Fullana, A.; Yoshikawa, K. Ash behavior during hydrothermal treatment for solid fuel applications. Part 1: Overview of different feedstock. *Energy Convers. Manag.* **2016**, *121*, 4022013408. [\[CrossRef\]](#)
- Heidari, M.; Dutta, A.; Acharya, B.; Mahmud, S. A review of the current knowledge and challenges of hydrothermal carbonization for biomass conversion. *J. Energy Inst.* **2018**. [\[CrossRef\]](#)
- Heidari, M.; Norouzi, O.; Salaudeen, S.A.; Acharya, B.; Dutta, A. Prediction of hydrothermal carbonization with respect to the biomass components and severity factor. *Energy Fuels* **2019**. [\[CrossRef\]](#)
- Libra, J.A.; Ro, K.S.; Kammann, C.; Funke, A.; Berge, N.D.; Neubauer, Y.; Titirici, M.-M.; Fühner, C.; Bens, O.; Kern, J.; et al. Hydrothermal carbonization of biomass residuals: A comparative review of the chemistry, processes and applications of wet and dry pyrolysis. *Biofuels* **2011**, *2*, 71–106. [\[CrossRef\]](#)
- Morandi, F.; Perrin, A.; Østergård, H. Miscanthus as energy crop: Environmental assessment of a miscanthus biomass production case study in France. *J. Clean. Prod.* **2016**, *137*, 313–321. [\[CrossRef\]](#)
- Kambo, H.S.; Dutta, A. A comparative review of biochar and hydrochar in terms of production, physico-chemical properties and applications. *Renew. Sustain. Energy Rev.* **2015**, *45*, 359–378. [\[CrossRef\]](#)
- Kambo, H.S.; Dutta, A. Comparative evaluation of torrefaction and hydrothermal carbonization of lignocellulosic biomass for the production of solid biofuel. *Energy Convers. Manag.* **2015**, *105*, 746–755. [\[CrossRef\]](#)
- Kambo, H.S.; Dutta, A. Strength, storage, and combustion characteristics of densified lignocellulosic biomass produced via torrefaction and hydrothermal carbonization. *Appl. Energy* **2014**, *135*, 182–191. [\[CrossRef\]](#)
- Mihajlović, M.; Petrović, J.; Maletić, S.; Isakovski, M.K.; Stojanović, M.; Lopičić, Z.; Trifunović, S. Hydrothermal carbonization of Miscanthus × giganteus: Structural and fuel properties of hydrochars and organic profile with the ecotoxicological assessment of the liquid phase. *Energy Convers. Manag.* **2018**, *159*, 254–263. [\[CrossRef\]](#)
- Smith, A.M.; Whittaker, C.; Shield, I.; Ross, A.B. The potential for production of high quality bio-coal from early harvested Miscanthus by hydrothermal carbonisation. *Fuel* **2018**, *220*, 546–557. [\[CrossRef\]](#)
- Jenie, S.N.A.; Kristiani, A.; Kustomo; Simanungkalit, S.; Mansur, D. Preparation of nanobiochar as magnetic solid acid catalyst by pyrolysis-carbonization from oil palm empty fruit bunches. *AIP Conf. Proc.* **2017**, *1904*. [\[CrossRef\]](#)
- Demirbas, A. Effects of temperature and particle size on bio-char yield from pyrolysis of agricultural residues. *J. Anal. Appl. Pyrolysis* **2004**, *72*, 243–248. [\[CrossRef\]](#)
- Singh, K.; Sivanandan, L. Hydrothermal Carbonization of Spent Osmotic Solution (SOS) Generated from Osmotic Dehydration of Blueberries. *Agriculture* **2014**, *4*, 239–259. [\[CrossRef\]](#)
- Gamgoum, R.; Dutta, A.; Santos, R.; Chiang, Y. Hydrothermal Conversion of Neutral Sulfite Semi-Chemical Red Liquor into Hydrochar. *Energies* **2016**, *9*, 435. [\[CrossRef\]](#)
- ASTM. *ASTM D5142-09, Standard Test. Methods for Proximate Analysis of the Analysis Sample of Coal and Coke by Instrumental* ProcASTM D5142-09; ASTM Int.: West Conshohocken, PA, USA, 2009. [\[CrossRef\]](#)
- Kambo, H.S. Energy Densification of Lignocellulosic Biomass via Hydrothermal Carbonization and Torrefaction. Master's Thesis, University of Guelph, Guelph, ON, Canada, 2014.
- Nizamuddin, S.; Baloch, H.A.; Griffin, G.J.; Mubarak, N.M.; Bhutto, A.W.; Abro, R.; Mazari, S.A.; Ali, B.S. An overview of effect of process parameters on hydrothermal carbonization of biomass. *Renew. Sustain. Energy Rev.* **2017**, *73*, 1289–1299. [\[CrossRef\]](#)

-
28. Zhang, B.; Heidari, M.; Regmi, B.; Salaudeen, S.; Arku, P.; Thimmannagari, M.; Dutta, A. Hydrothermal Carbonization of Fruit Wastes: A Promising Technique for Generating Hydrochar. *Energies* **2018**, *11*, 2022. [[CrossRef](#)]
 29. Oo, A.; Kelly, J.; Lalonde, C. Assessment of Business Case for Purpose-Grown Biomass in Ontario. Available online: <https://reseauquebecoisdesaeroports.ca/wp-content/uploads/11h00-Christian-Perreault-Assessment-of-business-case-for-purpose-grown-biomass-in-ontario-march-2012.pdf> (accessed on 1 March 2012).